

Best analytical practices for estimating consumer reliance on basal food sources using bulk stable isotopes

Mattia Ghilardi^{1,*}, Renato A. Morais¹, Simon J. Brandl², Jordan M. Casey²,
Alexandre Mercière¹, Fabien Morat¹, Nina M. D. Schiettekatte³, Mohsen
Kayal^{4,5}, Yves Letourneur⁶, Valeriano Parravicini¹

¹PSL Université Paris, CRIOBE, EPHE-CNRS-UPVD, 58 Avenue Paul Alduy, 66100 Perpignan,
France

²Department of Marine Science, The University of Texas at Austin, Marine Science Institute, 750
Channel View Drive, 78373 Port Aransas, Texas, USA

³MARE – Marine and Environmental Sciences Centre & ARNET – Aquatic Research
Infrastructure Network Associated Laboratory, Laboratório Marítimo da Guia, Faculdade de
Ciências, Universidade de Lisboa, Cascais, Portugal

⁴UMR Entropie (IRD-IFREMER-UR-UNC), BP A5, 98848 Nouméa, New Caledonia

⁵Station Marine d'Endoume, Marseille, France

⁶UMR Entropie (IRD-IFREMER-UR-UNC), EMR SantEco, Université de la Nouvelle Calédonie,
BP R4, 98851 Nouméa cedex, New Caledonia

*Corresponding author: mattia.ghilardi91@gmail.com

Abstract

1. Bulk stable isotopes have been utilised by ecologists for decades to trace the assimilation of basal food sources across trophic positions. However, there is a lack of guidance on the post-laboratory analytical workflow, leading to inconsistencies in how isotopic data are processed and interpreted.
2. We provide a comprehensive description of this necessary post-laboratory analytical workflow, including the mathematical rationale underlying the estimation of consumer reliance on basal sources. Using simulated data, we test the sensitivity of estimated basal source proportions to the number of isotopic baselines used for the estimation of consumer trophic position and to varying sample sizes of sources and consumers. Finally, we apply the workflow to a coral reef food web to quantify fish reliance on benthic and pelagic primary production.
3. Our results indicate that estimated basal source proportions are highly sensitive to bias in the estimation of consumer trophic position, suggesting that trophic position estimation requires careful consideration of the number and nature of selected isotopic baselines. We provide an R function to quantify this bias. By contrast, the precision and uncertainty—but not the accuracy—of these proportions are influenced by the sample sizes of consumers and sources. Thus, small sample sizes can still yield valid estimations and can be included. The case study further highlights the sensitivity of estimated proportions to the selection of

36 trophic discrimination factors (TDFs), and we suggest performing a sensitivity analysis with
37 alternative TDFs.

38 4. While compound-specific stable isotope analysis is gaining prominence, bulk stable
39 isotope analysis remains a cornerstone for field ecologists due to its high throughput,
40 cost-effectiveness and availability of data collected over the last 20 years. By providing a
41 detailed analytical framework and identifying future directions for model development, we
42 offer a robust analytical foundation for future isotopic studies.

43 **Keywords:** mixing models, trophic position, trophic discrimination factors, food web
44 analysis, methodological framework, resource assimilation, isotope ecology

45 1 Introduction

46 Tracing energy and matter across food webs has been a central endeavour since Lindeman's
47 (1942) seminal study on trophodynamics. Declining cost for the analysis of biotracers (i.e.,
48 biological markers such as stable isotopes and fatty acids; Appendix S1) and the advancement
49 of statistical methods (e.g., quantitative fatty acid signature analysis and stable isotope
50 mixing models [SIMMs] used to estimate proportional source contributions to consumers;
51 Appendix S1) have facilitated their application in ecological research, including in large-
52 scale monitoring efforts conducted by non-specialists (e.g., Bird et al., 2018; Lorrain et al.,
53 2020; Pethybridge et al., 2018). Consequently, standardised guidance on biotracer data
54 and modelling procedures has become essential. While foundational work has established
55 best practices for the general use of SIMMs in food web studies (e.g., Phillips et al., 2014),
56 there remains a lack of clear guidance regarding the post-laboratory analytical workflow for
57 using bulk stable isotopes to estimate consumer reliance on basal food sources (i.e., primary
58 producers and particulate organic matter) across trophic positions (i.e., a continuous measure
59 of an organism's position in a food web; Appendix S1).

60 Over the past few decades, stable isotope analysis (SIA; the measurement of the relative
61 isotopic abundance of elements within a sample; Appendix S1) has become a primary tool for
62 the study of bulk tissues in animal ecology (Gannes et al., 1997; Martínez del Rio et al., 2009).
63 The standardisation of laboratory protocols has led to the vast accumulation of experimen-
64 tal and field data (Martínez del Rio et al., 2009), facilitating the development of Bayesian
65 SIMMs to reconstruct animal diets and trace basal source contributions (e.g., Ferger et al.,

66 2013; Garcia et al., 2018; Hilting et al., 2013; McMahon et al., 2021; Moustaka et al., 2024;
67 Reid et al., 2008; Santos et al., 2020; Solomon et al., 2011; Zapata-Hernández et al., 2021).
68 While other more accurate biotracer methods such as compound-specific isotope analysis are
69 increasingly used to study animal diets (Nielsen et al., 2018; Pickett et al., 2024), their appli-
70 cation is constrained by high financial costs, time-consuming and highly-specialised sample
71 processing (Vane et al., 2025); therefore, bulk SIA remains the mainstream approach. How-
72 ever, accurately interpreting bulk SIA data requires addressing several confounding factors,
73 such as isotopic variability at the base of the food web and trophic discrimination factor
74 (TDF; the difference in isotopic values between consumer tissues and their diet; Appendix
75 S1), as isotopic values are influenced by both the consumer’s environment and its physiolog-
76 ical processing of nutrients (Martínez del Rio et al., 2009).

77 Estimating the contribution of basal sources to secondary or higher-order consumers
78 using bulk SIA and SIMMs requires consumer signatures to be corrected for total trophic
79 discrimination between them and the food web base (Reid et al., 2008). This necessitates
80 accurate estimates of consumer trophic positions and TDFs of individual trophic steps, in-
81 troducing multiple sources of error. While total discrimination can be directly calculated for
82 simplified food webs by summing the TDFs of each trophic link (Pickett et al., 2024; Reid
83 et al., 2008), the standard approach for more complex food webs is to multiply an average
84 TDF per trophic step by the number of trophic steps between consumers and basal sources
85 (i.e., their difference in trophic position) (Phillips et al., 2014). This approach assumes
86 that discrimination remains constant across trophic levels—an assumption rarely verified.
87 In addition, a thorough evaluation of its mathematical rationale and sensitivity to trophic
88 position estimation is currently lacking. Most studies address this by using either literature-
89 derived trophic position values (e.g., Hilting et al., 2013) or estimates derived from one or
90 two isotopic baselines (i.e., the isotopic composition of a basal component of a food web;
91 Appendix S1), such as primary consumers (e.g., Zapata-Hernández et al., 2021) or the mean
92 $\delta^{15}\text{N}$ of all primary producers (e.g., Ferger et al., 2013; Garcia et al., 2018; Moustaka et al.,
93 2024). However, the impact of these methodological choices on the resulting source propor-
94 tions is frequently unknown, highlighting the need for a detailed evaluation of the analytical
95 workflow.

96 Here, we describe a comprehensive workflow to estimate consumer reliance on basal food
97 sources using bulk SIA of carbon and nitrogen (and potentially other elements such as sulfur
98 or hydrogen) and provide the mathematical rationale underpinning this approach. Using
99 simulated data, we: (1) test the accuracy of the analytical workflow when using one or
100 two baselines to estimate consumer trophic position; and (2) investigate how the estimated
101 proportional contributions of sources are affected by consumer or source sample sizes. Finally,
102 we illustrate this analytical workflow using a case study of a coral reef food web in Mo'orea,
103 French Polynesia, estimating the reliance of 194 coral reef fish species on pelagic (external)
104 and benthic (internal) primary production.

105 **2 Materials and Methods**

106 **2.1 Analytical workflow and mathematical rationale**

107 Estimating consumer reliance on basal food sources using bulk SIA relies on a core mathe-
108 matical principle: the stable isotope value of a mixture (e.g., consumer tissue) is determined
109 by the proportional contributions of its sources and their respective stable isotope values.
110 This general SIMM is expressed as:

$$y_j = \sum_{k=1}^K p_k \mu_{jk}, \quad (1)$$

111 where y_j is the stable isotope value of the mixture for the j^{th} isotope, μ_{jk} is the mean stable
112 isotope value of the k^{th} source (of K total sources), and p_k is the proportional contribution
113 of the k^{th} source to the mixture, such that $\sum_{k=1}^K p_k = 1$.

114 To apply this model to animal diet and food web analysis, the mean isotopic values of
115 food sources must be corrected for trophic discrimination:

$$y_j = \sum_{k=1}^K p_k (\mu_{jk} + \Lambda_{jk}), \quad (2)$$

116 where Λ_{jk} is the total TDF accumulated between the consumer and the k^{th} source for the
117 j^{th} isotope.

118 Directly measuring Λ_{jk} is generally impractical for higher-order consumers (TP > 2),
119 as it requires feeding experiments spanning multiple trophic links. This framework resolves
120 this limitation via a three-step analytical workflow: (1) estimating consumer trophic position
121 relative to isotopic baselines; (2) mathematically rescaling consumer isotopic values to the
122 food web base to remove accumulated discrimination; and (3) fitting Bayesian SIMMs to the
123 rescaled data to estimate proportional contributions of basal sources (Figure 1).

124 2.1.1 Preliminary steps: Data preparation

125 1. *$\delta^{13}\text{C}$ lipid correction.* Prior to analysis, carbon stable isotope data must be evaluated
126 for lipid-derived bias. Lipids are significantly depleted in ^{13}C compared to proteins
127 and carbohydrates (DeNiro & Epstein, 1977; McConnaughey & McRoy, 1979), mean-
128 ing high variability in lipid content among organisms and tissues can confound source
129 proportion estimations (Kiljunen et al., 2006). Animal tissue samples (consumers and
130 baselines) with high lipid content, typically indicated by C:N ratios >3.5 (Post et
131 al., 2007), should be corrected either through chemical lipid extraction during sam-
132 ple preparation or via mathematical normalisation of $\delta^{13}\text{C}$ values using established
133 equations based on C:N ratios (e.g., Skinner et al., 2016 for fish tissues). For plant
134 samples (basal sources), extraction or normalisation should be performed on samples
135 with >40% carbon, and normalisation should be based on percent carbon rather than
136 the C:N ratio (Post et al., 2007). Correcting carbon signatures from the outset prevents
137 lipid-induced noise from propagating through the analytical workflow.

138 2. *Selection of basal sources.* The number of basal sources (K) must be carefully man-
139 aged. While all relevant sources should ideally be included—an implicit but rarely met
140 assumption in any mixing model—exceeding the $n + 1$ limit (where n is the number
141 of stable isotopes) creates an underdetermined system lacking an exact analytical solu-
142 tion. Bayesian SIMMs, however, provide probabilistic solutions for underdetermined
143 systems, but often yield broad, multimodal posterior distributions because multiple,
144 disparate source combinations can produce identical consumer signatures (Osada et
145 al., 2021; Phillips et al., 2014; Stock et al., 2018). To improve model inference, re-

146 searchers may group sources *a priori* based on isotopic similarity, thereby reducing
 147 the number of possible analytical solutions, or aggregate their estimated proportions *a*
 148 *posteriori* based on functional similarity, potentially yielding more constrained results
 149 (see Phillips et al., 2005; Phillips et al., 2014; Stock et al., 2018).

150 3. *Selection of isotope-specific TDFs* (λ_j). This framework assumes constant discrimi-
 151 nation across trophic levels, meaning total discrimination (Λ_{jk}) is the product of the
 152 TDF of a single trophic step (λ_{jk}) and the difference in trophic position between the
 153 consumer (TP_c) and the k^{th} source (TP_k) (Phillips et al., 2014):

$$\Lambda_{jk} = \lambda_{jk}(TP_c - TP_k). \quad (3)$$

154 Because source-specific values (λ_{jk}) are generally unknown for primary producers, they
 155 are replaced by a common isotope-specific TDF (λ_j) obtained from meta-analyses (e.g.,
 156 $0.39 \pm 1.3\%$ for $\delta^{13}C$ and $3.4 \pm 0.98\%$ for $\delta^{15}N$, Post, 2002), ideally matched to tissue
 157 and taxonomic groups. When all k sources represent the base of the food web ($TP_k =$
 158 1), the equation simplifies to:

$$\Lambda_{jk} = \Lambda_j = \lambda_j(TP_c - 1). \quad (4)$$

159 While discrimination varies across individual feeding links (Canseco et al., 2022; Caut
 160 et al., 2009; Stephens et al., 2023), using an average stepwise TDF (λ_j) provides a
 161 consistent discrimination across multiple trophic transfers and is considered a robust
 162 approximation when integrated across the diverse pathways of an entire food web
 163 (Post, 2002). Substituting Equation 4 into Equation 2 yields the foundational workflow
 164 equation:

$$y_j = \sum_{k=1}^K p_k(\mu_{jk} + \lambda_j(TP_c - 1)). \quad (5)$$

165 4. *Selection of isotopic baselines*. Rather than primary producers, long-living primary
 166 consumers (e.g., grazers, filter feeders) should be used as isotopic baselines to inte-
 167 grate baseline temporal variations (Cabana & Rasmussen, 1996; Post, 2002; Vander

168 Zanden & Rasmussen, 1999, 2001). The suitability of these baselines should be verified
 169 by estimating their basal source contributions via SIMMs. While this verification is
 170 often completed *a posteriori*, it provides a critical diagnostic check on whether the
 171 chosen baselines align with the intended trophic pathways. If a baseline consumer,
 172 assumed to represent a specific pathway (e.g., benthic), is found to derive most of
 173 its energy from an alternative pathway (e.g., pelagic), its baseline status is violated.
 174 When consumers derive energy from multiple discrete pathways (e.g., benthic-pelagic,
 175 terrestrial-aquatic), multiple baseline consumers are required (Post, 2002).

176 **2.1.2 Step 1: Estimating consumer trophic position (TP_c)**

177 To solve Equation 5, consumer trophic position (TP_c) must be estimated relative to either one
 178 or two isotopic baselines using models derived from the general mixing model (Equation 2):

- 179 • *One-baseline model.* When a single baseline consumer represents the food web base,
 180 TP_c can be estimated using a single isotope, typically δ¹⁵N (Cabana & Rasmussen,
 181 1996; Post, 2002). In this framework, Equation 2 becomes

$$\delta^{15}\text{N}_c = \delta^{15}\text{N}_b + \lambda_{\text{N}}(\text{TP}_c - \text{TP}_b), \quad (6)$$

182 which, rearranged to solve for TP_c, gives

$$\text{TP}_c = \text{TP}_b + \frac{\delta^{15}\text{N}_c - \delta^{15}\text{N}_b}{\lambda_{\text{N}}}, \quad (7)$$

183 where TP_b represents the trophic position of the baseline and λ_N is the isotope-specific
 184 TDF for δ¹⁵N.

- 185 • *Two-baseline model.* In systems with two distinct trophic pathways, a dual-baseline,
 186 dual-isotope mixing model (δ¹³C and δ¹⁵N) solves for both TP_c and the proportional
 187 contribution of the two baselines that typically have an identical trophic position (TP_{b1}
 188 = TP_{b2} = TP_b) (Quezada-Romegialli et al., 2018):

$$\delta^{15}\text{N}_c = p\delta^{15}\text{N}_{b1} + (1 - p)\delta^{15}\text{N}_{b2} + \lambda_{\text{N}}(\text{TP}_c - \text{TP}_b) \quad (8)$$

$$\delta^{13}\text{C}_c = p\delta^{13}\text{C}_{b1} + (1 - p)\delta^{13}\text{C}_{b2} + \lambda_C(\text{TP}_c - \text{TP}_b), \quad (9)$$

189 Under this model, TP_c is estimated by accounting for the isotopic signatures of both
 190 baselines:

$$\text{TP}_c = \text{TP}_b + \frac{\delta^{15}\text{N}_c - p\delta^{15}\text{N}_{b1} - (1 - p)\delta^{15}\text{N}_{b2}}{\lambda_N}, \quad (10)$$

191 where the proportional contribution of the first baseline (p) can be expressed as

$$p = \frac{\delta^{13}\text{C}_c - \delta^{13}\text{C}_{b2} - \lambda_C(\text{TP}_c - \text{TP}_b)}{\delta^{13}\text{C}_{b1} - \delta^{13}\text{C}_{b2}}, \quad (11)$$

192 and λ_C is the isotope-specific TDF for $\delta^{13}\text{C}$.

193 These models are the most frequently used across the literature (Kjeldgaard et al., 2021),
 194 and traditional point-estimate calculations have recently been replaced by Bayesian models
 195 that propagate parameter uncertainty into the TP_c estimation (e.g., the R package *tRophic-*
 196 *Position*, Quezada-Romegialli et al., 2018), providing a more modern and robust approach.

197 While these equations rely on constant discrimination, an alternative framework account-
 198 ing for systematic decreases in TDF values at higher trophic levels (Hussey et al., 2014) is
 199 detailed in Appendix S2.

200 2.1.3 Step 2: Isotopic rescaling of consumers

201 Once TP_c is estimated, the raw isotopic signature of each individual consumer (y_j) is math-
 202 ematically rescaled to the food web base (y_j^*) by rearranging Equation 5:

$$y_j^* = y_j - \lambda_j(\text{TP}_c - 1) = \sum_{k=1}^K p_k \mu_{jk}. \quad (12)$$

203 This transformation isolates y_j^* , representing the consumer's signature as if it fed directly
 204 at the base of its food web ($\text{TP} = 1$), thus stripping away the confounding effect of accu-
 205 mulated trophic discrimination. Standard Bayesian SIMMs cannot process individual-level
 206 uncertainty in consumer signatures during source contribution estimation, preventing uncer-
 207 tainty in trophic position and discrimination from propagating into the rescaled signatures
 208 (y_j^*). Consequently, the mean of the TDF (λ_j) and the mode of the estimated TP_c posterior

209 distribution are used as point estimates for this step. The mode is selected because it pro-
210 vides a more robust measure of central tendency than the mean or median when consumer
211 sample sizes are small and the posterior distribution exhibits non-normal geometry.

212 **2.1.4 Evaluation step: Mixing model validation**

213 Before implementing the final mixing models, the rescaled consumer values (y_j^*) and raw
214 basal source signatures must be plotted together in isospace to ensure that the consumer sig-
215 natures fall within the boundaries of the mixing polygon defined by the basal sources, so that
216 mathematically valid source contribution solutions exist (Phillips et al., 2014). If consumers
217 fall consistently outside, researchers must systematically re-evaluate the preliminary steps
218 to identify missing basal sources or more appropriate baselines and TDFs. Conversely, if
219 only isolated individuals fall outside the mixing polygon, they should be flagged as potential
220 outliers. Because extreme values can cause model convergence issues despite the integrated
221 error structures of Bayesian SIMMs that account for natural isotopic variation, a probabilis-
222 tic framework (e.g., Smith et al., 2013) can be employed to quantify the probability that
223 an individual's isotopic signature is explained by the model. An extremely low probability
224 indicates that the individual cannot be modelled by the sources at hand. Rather than serv-
225 ing as an automatic rule for exclusion, this metric provides a diagnostic check; the ultimate
226 decision whether to exclude the outliers and continue the inference, collect additional basal
227 source data to expand the polygon, or abort the analysis entirely rests with the researcher.
228 Regardless of the initial results, performing sensitivity analyses with alternative baselines or
229 TDFs remains good practice. Additionally, computing the normalised surface area of the
230 mixing polygon (Brett, 2014) using the *calc_area()* function in R package *MixSIAR* (Stock
231 et al., 2018) may be useful to detect weakly informative model geometry caused by poor
232 source separation or high source variance.

233 **2.1.5 Step 3: Estimating basal source proportions (p_k)**

234 Finally, a Bayesian SIMM is fitted to the rescaled consumer values (y_j^*) and the isotopic
235 signatures of basal sources to estimate the proportional contributions (p_k). Because all
236 accumulated trophic discrimination was accounted for and removed in step 2, the TDFs

237 within the mixing model must be explicitly set to zero (mean = 0, SD = 0).

238 Models can initially be run using a “uninformative”, generalist prior implying that all
239 source combinations are equally likely (i.e., a symmetric Dirichlet distribution where all
240 hyperparameters $\alpha_k = 1$). If the model exhibits poor convergence or yields biologically
241 unrealistic results, informative priors should be constructed using expert system knowledge
242 of the system or literature estimates. For example, for specialist consumers with clear trophic
243 affinities (e.g., grazing herbivores, or planktivores), it is sensible to assign a higher prior
244 weight (α_k) to the basal source representing the primary pathway, while decreasing the
245 weights of alternative sources. To prevent these priors from overriding the actual stable
246 isotope data, the Dirichlet hyperparameters should be rescaled so that their sum equals the
247 total number of sources (K , Stock et al., 2018).

248 These models can be fitted using Markov Chain Monte Carlo (MCMC) or Fixed Form
249 Variational Bayes algorithms across several R packages such as *MixSIAR* (Stock et al., 2018),
250 *simmr* (Govan et al., 2023), or *cosimmr* (Govan et al., 2024). Among these, MixSIAR is cur-
251 rently the most feature-rich, allowing for the inclusion of covariates, hierarchical structures,
252 and diverse error formulations (Stock et al., 2018).

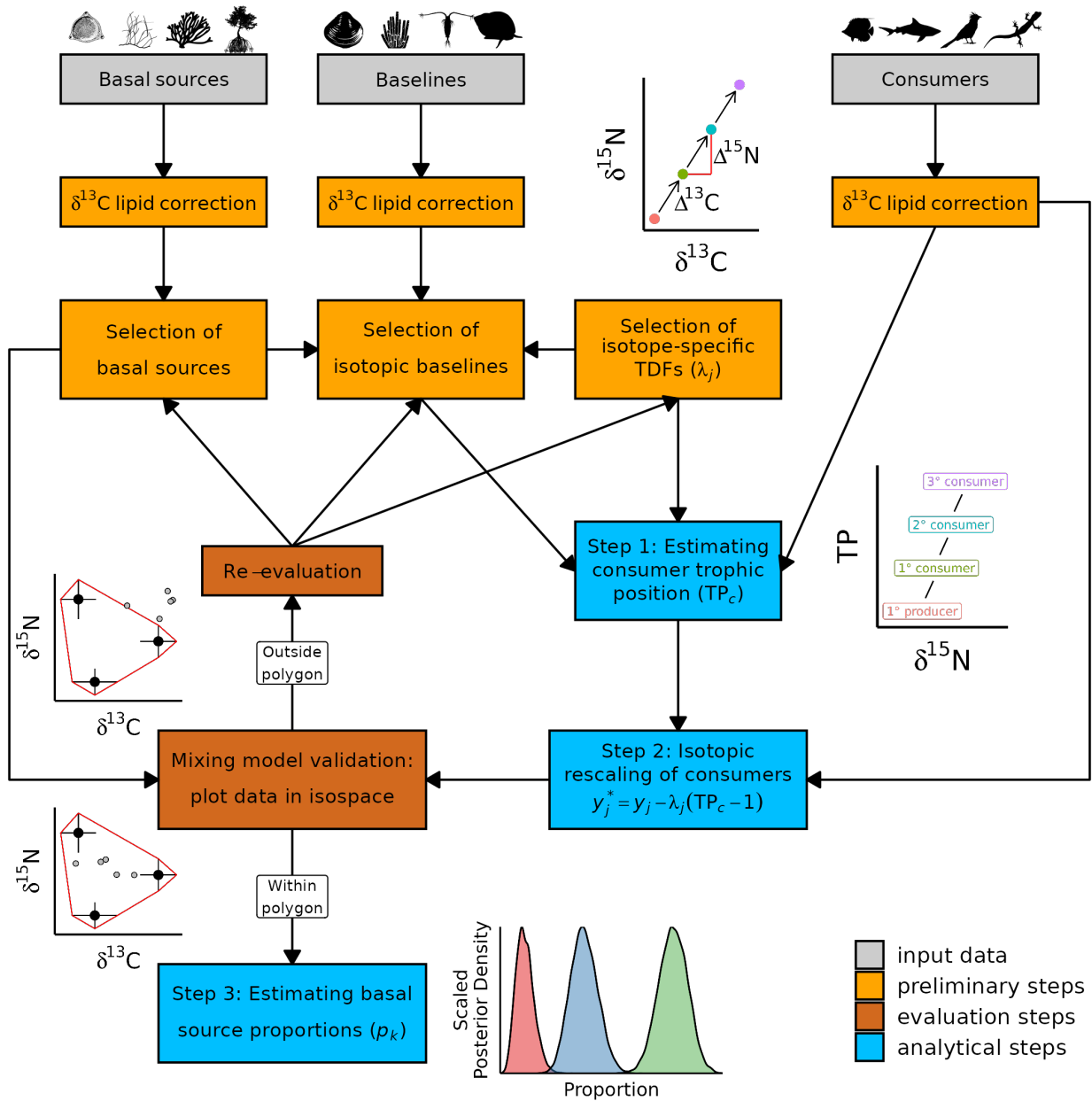


Figure 1: Flowchart for the estimation of consumer reliance on basal sources, made with the R package *ggflowchart* (Rennie, 2023). The depicted workflow is valid for both assumptions of constant and narrowing discrimination across trophic levels (see Appendix S2). Silhouettes from <https://www.phylopic.org/> and contributed by Emily Jane McTavish, Rachel Wooliver, Guillaume Dera, Pablo Amador Crespo, Marina Vingiani, Alexandra Hahn, perevolotsky, John Hlavin, Kai Caspar, and Jose Carlos Arenas-Monroy.

253 2.2 Simulations

254 To evaluate the performance of the proposed workflow across different ecological scenarios,
255 we conducted simulations using food webs where the “true” consumer trophic position (TP_c)
256 and basal source proportions (p_k) were known. Specifically, we used these simulated food
257 webs to: (1) test the accuracy of the workflow in estimating the proportional contribution
258 of basal sources using one or two isotopic baselines for the estimation of consumer trophic
259 position, and (2) investigate how consumer and source sample sizes influence the precision,
260 uncertainty, and accuracy of the estimated proportions. These simulations allow for a quan-
261 titative assessment of the workflow’s sensitivity to baseline configuration and sampling effort.

262 2.2.1 Simulation design and data generation

263 We carried out all simulations for a two-isotope system ($\delta^{13}\text{C}$ and $\delta^{15}\text{N}$) consisting of three
264 basal sources, one or two isotopic baselines, and one consumer. The data generation pro-
265 cess described below was implemented using the custom R function *simulate_food_web()*
266 (available in Appendix S3).

267 For each isotope, source standard deviations were generated from a uniform distribution,
268 $U(0.5, 1.5)$. Source means were randomly sampled without replacement from a vector of six
269 equally spaced values—twice the number of sources—between -10 and 10 (i.e., -10, -6, -2,
270 2, 6, 10), avoiding collinearity between isotopes (Schwarcz, 1991). This sampling strategy
271 ensures that sources have isotopically distinct signatures (Gannes et al., 1998), which cannot
272 be assumed when sampling from a probability distribution as in previous simulation studies
273 (Semmens et al., 2009; Stock & Semmens, 2016).

274 Source proportions for baseline(s) and consumer were generated from Dirichlet distribu-
275 tions. A flat *Dirichlet*(1, 1, 1) was used for the consumer. For the one-baseline simulations,
276 a symmetric *Dirichlet*(10, 10, 10) was used to represent the common practice of using the
277 mean isotopic signature of all basal sources as a baseline (e.g., Ferger et al., 2013; Garcia
278 et al., 2018; Moustaka et al., 2024). For the two-baseline simulations, we used asymmetric
279 Dirichlet distributions to ensure that the baselines represented two distinct trophic pathways
280 (see Appendix S4: Figure S1). To satisfy the mixing models assumption that all sources con-

281 tribute to the consumer (i.e., all sources included will have an estimated relative contribution
282 exceeding zero, even if some do not significantly contribute to consumer nutrition), we con-
283 strained all source proportions to a minimum of 5% following Stock & Semmens (2016). This
284 was achieved with a linear transformation commonly used in Beta and Dirichlet regressions
285 (Douma & Weedon, 2019; Maier, 2014; Smithson & Verkuilen, 2006):

$$p^* = \frac{p(n-1) + \frac{1}{K}}{n}, \quad (13)$$

286 where p is the source proportion, K is the number of sources, and $n = \frac{1/K}{0.05} = 6.67$ for
287 three sources.

288 Baseline and consumer isotopic data were generated following Stock & Semmens (2016).
289 In practice, for each individual baseline and consumer, the number of samples taken from each
290 source was simulated using a multinomial distribution defined by the simulated proportions
291 and a total number of source items eaten (i.e., total consumption). The normal distribution
292 of each source, defined by its mean and standard deviation, was repeatedly sampled based
293 on these sample sizes. Isotopic values were calculated as the means of all source samples
294 plus a residual error from $N(0, 1)$.

295 To reflect the reduction in isotopic variance at higher trophic levels due to time averaging
296 (O'Reilly et al., 2002), we set a higher consumption for consumers than for baselines (40
297 vs. 20). These values serve as mathematical control for the variance of the simulated isotopic
298 data and have no direct biological scaling (Stock & Semmens, 2016).

299 Finally, the total trophic discrimination, $\lambda_j(\text{TP}_c - 1)$, was added to the generated isotopic
300 values of consumers and baselines. Carbon and nitrogen TDFs (λ_j) were taken from Post
301 (2002). Baseline trophic position was fixed at 2 (i.e., primary consumers), so their total
302 discrimination equals λ_j . For consumers, a population-level mean TP_c was sampled from a
303 truncated normal distribution, $TNormal(\mu, \sigma, 2, 5)$. By setting the truncation bounds at
304 2 and 5, the population mean was strictly constrained within this realistic ecological range.
305 The hyper-parameters of this distribution, $\mu \sim U(2.5, 4.5)$ and $\sigma \sim U(0.1, 0.3)$, represent the
306 trophic distribution of a higher taxonomic rank (e.g., family). Individual-level TP_c values
307 were then generated by sampling from this population mean with an additional standard

308 deviation of 0.05 to account for intra-population variability.

309 **2.2.2 Modelling and software settings**

310 We used the R packages *tRophicPosition* (Quezada-Romegialli et al., 2018) for TP_c estima-
311 tion and *MixSIAR* (Stock et al., 2018) for estimating basal source proportions. *tRophic-*
312 *Position* models were run for four chains, each with 4,000 iterations and a 2,000-iteration
313 burn-in. *MixSIAR* models were run for three parallel chains—utilising modified source code
314 to allow chain parallelisation—each with 100,000 iterations, a 50,000-iteration burn-in and a
315 thinning rate of 50. Unless otherwise specified, all *MixSIAR* models utilised a multiplicative
316 error structure (Residual \times Process error) to integrate both unexplained consumer isotopic
317 variability (residual error) and variance due to the sampling process (process error) (Stock &
318 Semmens, 2016). We used default, weakly informative priors for all simulations and checked
319 model convergence using Gelman-Rubin statistics (Gelman & Rubin, 1992).

320 **2.2.3 One vs two baselines**

321 To compare the performance of the workflow under different baseline configurations, we
322 conducted simulations using 100 “true” food web structures (Appendix S4: Figure S2). For
323 each simulation, the workflow was applied twice to the same underlying data: once using a
324 one-baseline configuration and once using a two-baseline configuration. This paired design
325 ensured that the food webs were identical in terms of basal sources and consumer data, such
326 that any differences in the resulting estimates could be attributed specifically to the baseline
327 configuration. All food web components comprised of 10 observations (“samples”).

328 Workflow performance across the resulting estimations ($n = 200$) was evaluated based
329 on two metrics: 1) the maximum absolute error between estimated and known true source
330 proportions (bound between 0 and 1), and 2) the coverage of the true source proportions
331 within the 95% credible interval (CI). We then fitted a Bayesian distributional multilevel
332 beta regression using the R package *brms* (Bürkner, 2017) to test for differences in both
333 the mean and precision of the maximum absolute error between the one-baseline and two-
334 baseline approaches. Furthermore, we used this model to investigate the extent to which the
335 absolute error in TP_c estimation propagated through the workflow to affect the final source

336 proportion estimates (see Appendix S4: Section 4.1 for model details).

337 **2.2.4 Sensitivity to consumer sample size**

338 To investigate the workflow’s sensitivity to consumer sampling effort, we used a single, fixed
339 simulated food web with a two-baseline configuration (Appendix S4: Figure S3) as the
340 reference scenario for all tests. Holding the source sample sizes constant at $n = 10$, we
341 simulated 100 datasets for each of five consumer sample sizes ($n = 1, 3, 5, 10, 20$). This
342 approach ensured that the underlying food web structure remained identical, allowing us to
343 isolate the effect of sampling effort on the workflow’s performance.

344 For cases where $n = 1$, a process-only error structure was required because residual
345 variance cannot be estimated from a single data point (Stock & Semmens, 2016); for all
346 other sample sizes, the standard multiplicative error structure was maintained. We evaluated
347 the effect of consumer sample size on two metrics: (1) the median and (2) the 95% CI
348 width of the estimated source proportions. To model these relationships, we fitted two
349 Bayesian distributional non-linear power models using the R package *brms* (Bürkner, 2017)
350 (see Appendix S4: Section 4.2 for model details). While $n = 1$ cases were excluded from the
351 power models due to the differing error structure, they were retained in the overall analysis
352 to provide a heuristic indication of bias and uncertainty in data-poor scenarios.

353 **2.2.5 Sensitivity to source sample size**

354 An identical approach was used to assess sensitivity to source sampling effort. Using the
355 same fixed, two-baseline food web (Appendix S4: Figure S3), we simulated 100 datasets for
356 each of five source sample sizes ($n = 1, 3, 5, 10, 20$), while holding the consumer sample size
357 constant at $n = 10$. As with the consumer sample size simulations, we evaluated the effect
358 of source sample size on the median and 95% CI width of the estimated source proportions
359 using Bayesian distributional non-linear power models (Appendix S4: Section 4.2). All $n =$
360 1 cases were excluded from the power models because source variance cannot be estimated
361 from a single value. These cases were nonetheless evaluated to determine the extent of bias
362 and uncertainty introduced when only a single representative value is available per source—a
363 limitation that can occur in field-based studies due to logistical constraints or when analysing

364 existing datasets where only a single mean or sample is available.

365 **2.3 Case study: Mo’orea coral reef fishes**

366 To demonstrate the empirical application and robustness of our three-step analytical work-
367 flow, we applied it to an extensive stable isotope database of coral reef fishes and their basal
368 food web components from Mo’orea, French Polynesia. The dataset contains stable isotope
369 compositions ($\delta^{13}\text{C}$ and $\delta^{15}\text{N}$) for a total of 1,375 individual fishes spanning 194 species
370 and 45 families collected across lagoon and reef slope habitats between 2016 and 2019. To
371 characterise the base of the underlying food web, representative samples of major macroalgal
372 groups, benthic cyanobacteria, oceanic particulate organic matter (POM), and invertebrate
373 primary consumers (serving as isotopic baselines) were collected from the same habitats in
374 2016. Initial Bayesian linear regressions confirmed that while minor interannual isotopic
375 variations occurred in some species, the direction of these variations was inconsistent across
376 taxa, justifying the aggregation and analysis of the entire multi-year dataset. A detailed
377 description of sample collection, laboratory processing, and statistical analysis is provided
378 in Appendix S5: Section 1.

379 Collections were performed using permit number 681/MCE/ENV delivered by the Gov-
380 ernment of French Polynesia.

381 The analysis followed all sequential steps of the proposed workflow:

382 1. *Data preparation and parameter selection.* To eliminate lipid-derived bias, $\delta^{13}\text{C}$
383 data were mathematically normalised based on individual C:N ratios, applying
384 taxon-specific models for fish and invertebrate samples. For the basal sources, five
385 initial categories (benthic cyanobacteria, green, brown, and red algae, and oceanic
386 POM) were evaluated in isospace. Brown and green algae exhibited substantial
387 isotopic overlap and were grouped a priori, reducing the system to four distinct
388 basal sources. To evaluate workflow sensitivity to parameter selection, we selected
389 two distinct sets of widely used literature TDFs: general, non-tissue-specific values
390 from Post (2002) and muscle tissue-specific values from McCutchan Jr et al. (2003).
391 Finally, two long-lived primary consumers—benthic grazing gastropods (*Monetaria*

392 spp.) and filter-feeding bivalves (*Limaria fragilis*)—were selected as isotopic baselines.
393 Their suitability was verified via a Bayesian SIMM fitted with *MixSIAR* (Stock et
394 al., 2018), which confirmed their high fidelity to their assumed pathways (substantial
395 pelagic reliance for bivalves and predominant benthic reliance for gastropods).

396 2. *Steps 1 and 2: Trophic position and rescaling.* To estimate trophic position for each
397 fish species, we fitted Bayesian two-baseline models using *tTrophicPosition* (Quezada-
398 Romegialli et al., 2018) using the validated baselines and selected TDFs. Then, the
399 raw isotopic signatures of individual fish were rescaled to the food web base using
400 the estimated trophic position modes and mean TDF values, removing the accumu-
401 lated trophic discrimination. Because these steps were executed independently for
402 non-tissue-specific and muscle tissue-specific TDFs, two separate rescaled fish datasets
403 were generated for all subsequent steps.

404 3. *Evaluation step.* Both rescaled fish datasets were plotted in bi-dimensional isospace to
405 determine whether consumers correctly fell within the mixing polygon. While the vast
406 majority of individuals fell within the polygon boundaries, isolated individuals falling
407 outside were evaluated using the probabilistic framework of Smith et al. (2013). Ob-
408 servations with an explanatory probability $<1\%$ (11 individuals for non-tissue-specific
409 and 23 for muscle tissue-specific TDFs, representing 0.8% and 1.7% of the total obser-
410 vations, respectively) were flagged and removed to prevent model convergence failures.
411 Furthermore, the calculated normalised surface area of the mixing polygon was 35.5
412 SD^2 , confirming a well-resolved source geometry (Brett, 2014).

413 4. *Step 3: Basal source proportions.* To accommodate their complex ecological and evolu-
414 tionary structure, the rescaled consumer datasets were partitioned into eight distinct
415 trophic guilds capturing the primary energetic pathways of the reef (Appendix S6).
416 Within each guild, we fitted alternative Bayesian SIMMs using a process-only error
417 structure with *MixSIAR* (Stock et al., 2018) to evaluate the relative effects of body
418 size and evolutionary history. For each guild, a suite of four models of descending
419 complexity was executed: (1) a full model incorporating taxonomy as a nested ran-
420 dom effect (species within family) and fish total length as a continuous covariate;

421 (2) a taxonomy-only model; (3) a length-only model; and (4) a null model. Models
422 were fit using informative Dirichlet priors constructed from expert system knowledge
423 (Parravicini et al., 2020), maintaining a hyperparameter sum equal to the number of
424 sources ($K = 4$). Final model selection was performed through leave-one-out cross
425 validation (Vehtari et al., 2017) and stacking weights (Yao et al., 2018). Estimated
426 proportions for all algal sources (green-brown combined and red algae) were aggregated
427 *a posteriori* to yield an overarching algal contribution. Finally, species-specific median
428 source proportions estimated with non-tissue-specific and muscle tissue-specific TDFs
429 were directly compared using Bayesian multivariate linear regressions fitted with *brms*
430 (Bürkner, 2017) to provide a comprehensive check on the sensitivity of our ecological
431 conclusions.

432 **2.4 Computational environment**

433 Simulations and analyses were performed in R version 4.4.2 (R Core Team, 2024), using
434 *targets* version 1.6.0 (Landau, 2021) as pipeline tool to manage the project workflow, *renv*
435 version 1.0.5 (Ushey & Wickham, 2024) for package management and *crew* version 0.10.2
436 (Landau, 2024) for parallel computing. Bayesian SIMMs were fitted with *tRophicPosition*
437 version 0.8.0 (Quezada-Romegialli et al., 2018) and *MixSIAR* latest development version
438 (commit 037978f) (Stock et al., 2018) in JAGS (Just Another Gibbs Sampler) version 4.3.2
439 (Plummer, 2003), while Bayesian regression models were fitted with *brms* version 2.21.0
440 (Bürkner, 2017) using CmdStan version 2.35.0 (Gabry et al., 2024; Stan Development Team,
441 2024) as backend.

442 **3 Results**

443 **3.1 Simulations**

444 **3.1.1 One vs two baselines**

445 The workflow performed similarly irrespective of the baseline configuration. The 95% CI
446 of estimated source proportions included 59% and 54% of the true source proportions ($n =$

447 300, 100 food webs \times 3 sources) for the one-baseline and the two-baseline configurations,
448 respectively. Maximum absolute errors in estimated source proportions ranged between 0.01
449 and 0.63, although 84% and 85% of all estimated source proportions had an absolute error
450 of <0.2 for the one-baseline and the two-baseline configurations, respectively (Figure 2A and
451 Appendix S4: Figure S5A). The maximum absolute error did not differ in either the mean
452 ($P_{One-baseline>Two-baselines} = 0.16$) or precision ($P_{One-baseline>Two-baselines} = 0.13$) between the
453 two approaches (Appendix S4: Figure S5B). Furthermore, the maximum absolute error in
454 estimated source proportions was strongly, positively related to the absolute error in esti-
455 mated consumer trophic position (TP_c , Figure 2A), with no difference in the slope between
456 the two approaches ($\beta = 0.74[0.65, 0.86]$ for one baseline and $\beta = 0.77[0.69, 0.86]$ for two
457 baselines, respectively, with $P_{One-baseline>Two-baselines} = 0.33$). As demonstrated in Appendix
458 S7, the error in estimated TP_c is proportional to the difference in TP-corrected $\delta^{15}N$ (i.e., at
459 $TP = 1$) between the consumer and the baseline(s) (Figure 2B), which results from different
460 contributions of the sources to the consumer and baseline(s).

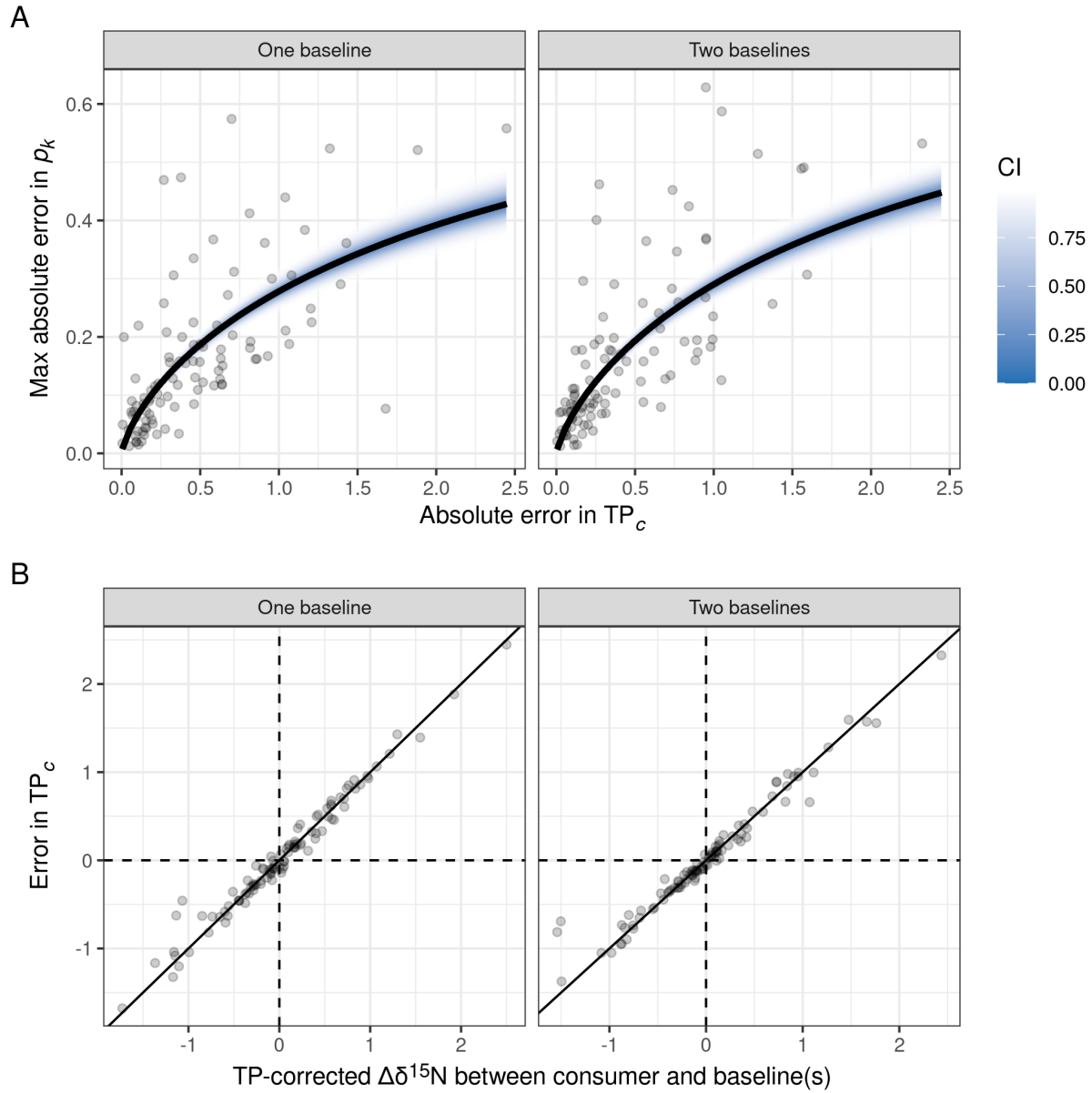


Figure 2: A) Relationship between the maximum absolute error in estimated source proportions (p_k) and the absolute error in estimated consumer trophic position (TP_c) using one or two isotopic baselines. Semi-transparent points are raw data, while solid lines and ribbons are model predictions that represent the median and credible interval (CI), respectively. B) Relationship between the error in estimated TP_c and the TP-corrected difference in $\delta^{15}N$ between the consumer and the baseline(s) for the one-baseline and two-baseline approaches. See appendix S7 for mathematical derivation. Semi-transparent points are raw data, while solid lines represent a 1:1 relationship.

461 3.1.2 Sensitivity to consumer sample size

462 In this food web (Appendix S4: Figure S3), the true source contributions to the simulated
463 consumer were relatively well recovered with small absolute errors (<0.1) in the estimates
464 (Figure 3A). Consumer sample size affected both the estimated median and the 95% CI width
465 of source proportions (Figure 3A-B). However, it only had a weak effect on the mean of the
466 estimated medians (i.e., accuracy), while the mean of the estimated 95% CI widths (i.e.,
467 uncertainty) strongly decreased with increasing sample size (Figure 3A-B and C-D, panel μ).
468 In addition, the variance of both estimates (i.e., precision) decreased with increasing sample
469 size (Figure 3C-D, panel σ). Note that the slightly different point estimates obtained with a
470 consumer sample size of one compared to larger sample sizes are likely due to different error
471 structures in the mixing model (i.e., Process-only vs Residual \times Process).

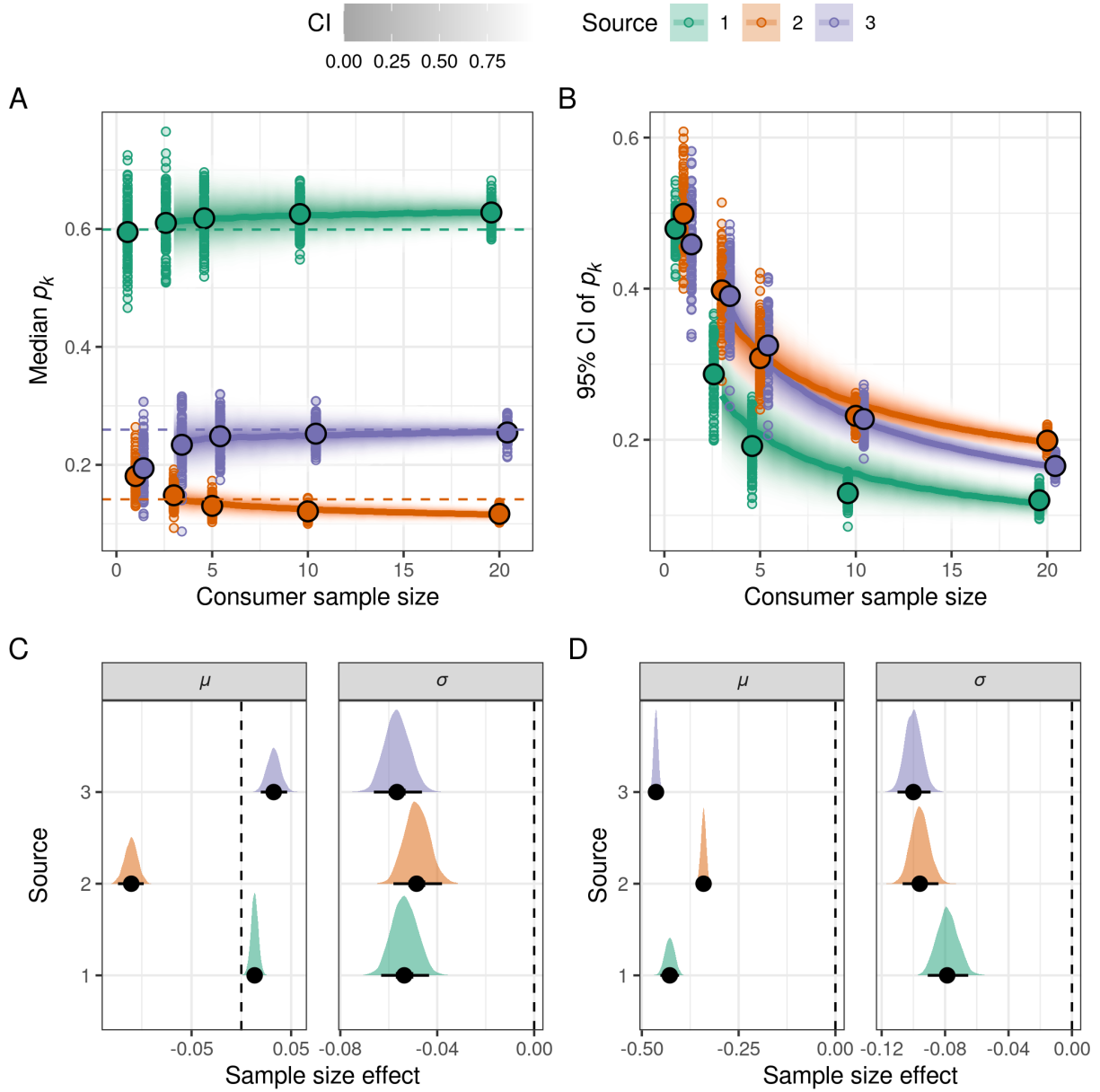


Figure 3: A-B) Relationships between the median and 95% credible interval (CI) width of source proportions (p_k) and consumer sample size. Small, coloured points are raw data, while large points represent the means. These are horizontally adjusted for clarity. Solid lines and ribbons are model predictions and represent the median and CI, respectively. Coloured dashed lines in A represent true p_k . C-D) Effect of consumer sample size on the mean (μ) and standard deviation (σ) of the median and 95% CI width of p_k , respectively. Black dots and intervals represent the median, 50 and 95% CI, respectively, while the coloured area represents the posterior density. Some intervals are too small to be seen. Vertical dashed lines depict 0 (i.e., no effect).

472 3.1.3 Sensitivity to source sample size

473 Source sample size did not affect the mean of the estimated median source proportions (i.e.,
474 accuracy) (Figure 4A and C, panel μ), but a larger source sample size reduced the mean of
475 the estimated 95% CI width of source proportions (Figure 4B and D, panel μ), although to a
476 smaller extent compared to the consumer sample size. Furthermore, a larger source sample
477 size reduced the variance of both estimates (i.e., precision) (Figure 4C-D, panel σ).

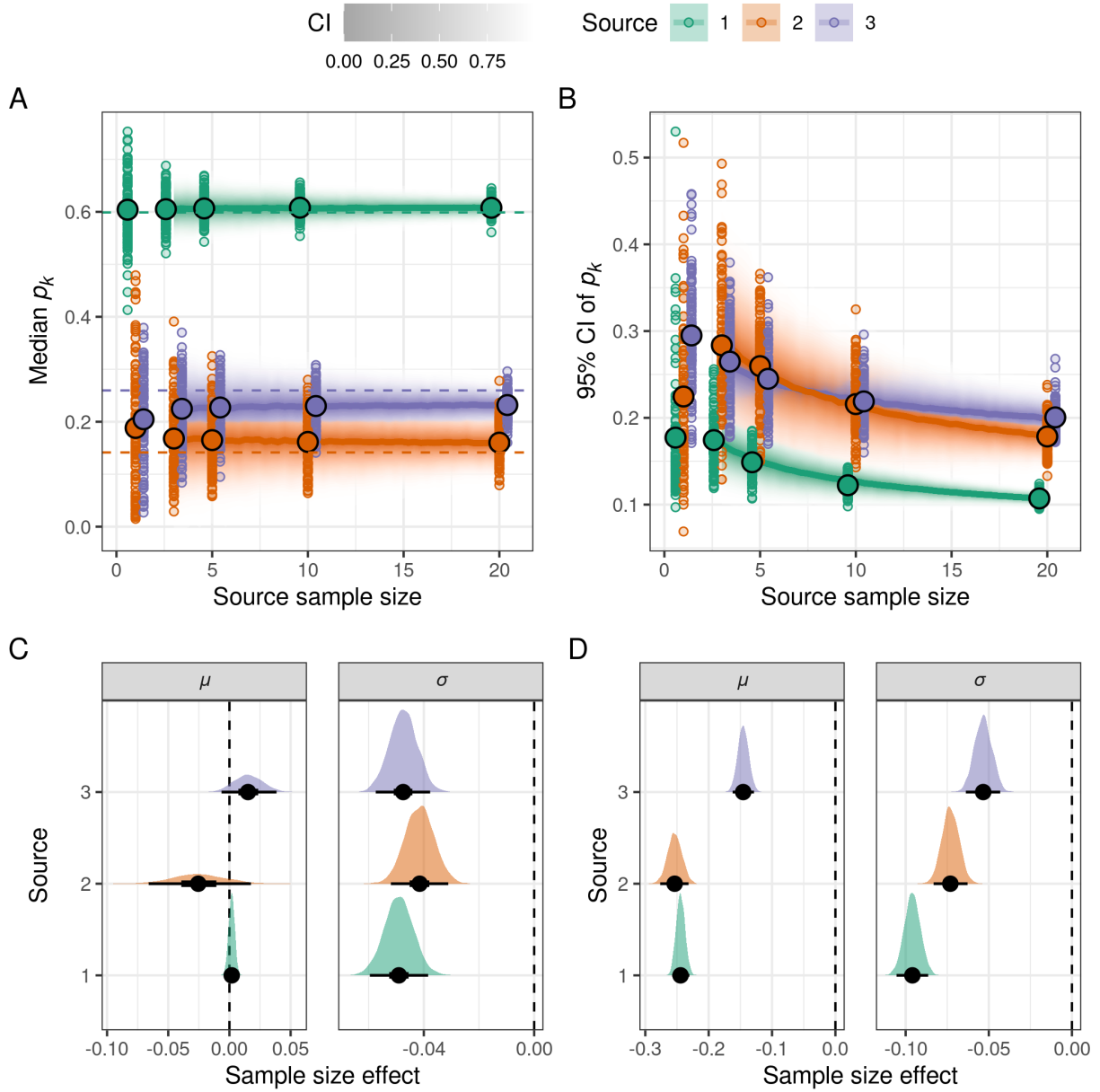


Figure 4: A-B) Relationships between the median and 95% credible interval (CI) width of source proportions (p_k) and source sample size. Small, coloured points are raw data, while large points represent the means. These are horizontally adjusted for clarity. Solid lines and ribbons are model predictions and represent the median and CI, respectively. Coloured dashed lines in A represent true p_k . C-D) Effect of source sample size on the mean (μ) and standard deviation (σ) of the median and 95% CI width of p_k , respectively. Black dots and intervals represent the median, 50 and 95% CI, respectively, while the coloured area represents the posterior density. Some intervals are too small to be seen. Vertical dashed lines depict 0 (i.e., no effect).

478 3.2 Case study

479 The selected models consistently included the full structure (including taxonomy and fish
480 total length) or only taxonomy (Appendix S5: Tables S5-S6). The estimated relative con-
481 tribution of basal sources to coral reef fishes in Mo'orea were strongly correlated between
482 the non-tissue-specific and muscle tissue-specific TDFs, with POM and algae (brown, green,
483 and red algae combined) providing the largest overall contributions to similar extents and
484 cyanobacteria providing the smallest contributions, regardless of the TDFs used (Appendix
485 S5: Figure S18A). However, the contribution of cyanobacteria was consistently higher using
486 non-tissue-specific TDFs than muscle tissue-specific ones, while the contributions of POM
487 were lower and those of algae showed no significant difference (Appendix S5: Figure S18B).
488 These differences were more pronounced for some trophic guilds than others (Appendix S5:
489 Figure S18C). Furthermore, the probability of fish falling within the mixing polygon was sim-
490 ilar when isotopic signatures were rescaled using non-tissue-specific or muscle tissue-specific
491 TDFs (Appendix S5: Figure S19), although fewer observations fell outside the mixing poly-
492 gon using non-tissue-specific TDFs than muscle tissue-specific ones (Appendix S5: Figures
493 S13-S14). Therefore, both TDFs appear appropriate for our study. We present the results
494 obtained with non-tissue-specific TDFs here and report those obtained with muscle tissue-
495 specific TDFs in Appendix S5.

496 On average, algae (brown, green, and red algae combined) were the dominant source
497 for herbivores and detritivores, benthic and sessile invertivores, and macrocarnivores; how-
498 ever, for sessile invertivores and macrocarnivores, the contribution of algae was only slightly
499 higher than that of POM (Figure 5). POM, however, was by far the dominant source for
500 omnivores and planktivores, contributing over 50% and highlighting their high reliance on
501 pelagic primary production. Cyanobacteria, despite having an overarching low contribution,
502 were the dominant source for microphages, indicating a high reliance on benthic microbial
503 primary production. These results are consistent with the known trophic ecology of these
504 fishes (Clements et al., 2017; McMahon et al., 2016; Parravicini et al., 2020). However, the
505 relative contribution of basal sources varied with fish body size for all trophic guilds except
506 benthic omnivores (Appendix S5: Figure S20), as well as across species and families for

507 all trophic guilds (Appendix S5: Figures S21-S28). Taxonomic variation was more marked
508 for some guilds (e.g., microphages) and less for others (e.g., planktivores). All results were
509 consistent using muscle tissue-specific TDFs (Appendix S5: Figures S29-S38), although the
510 estimated proportions differed in absolute values.

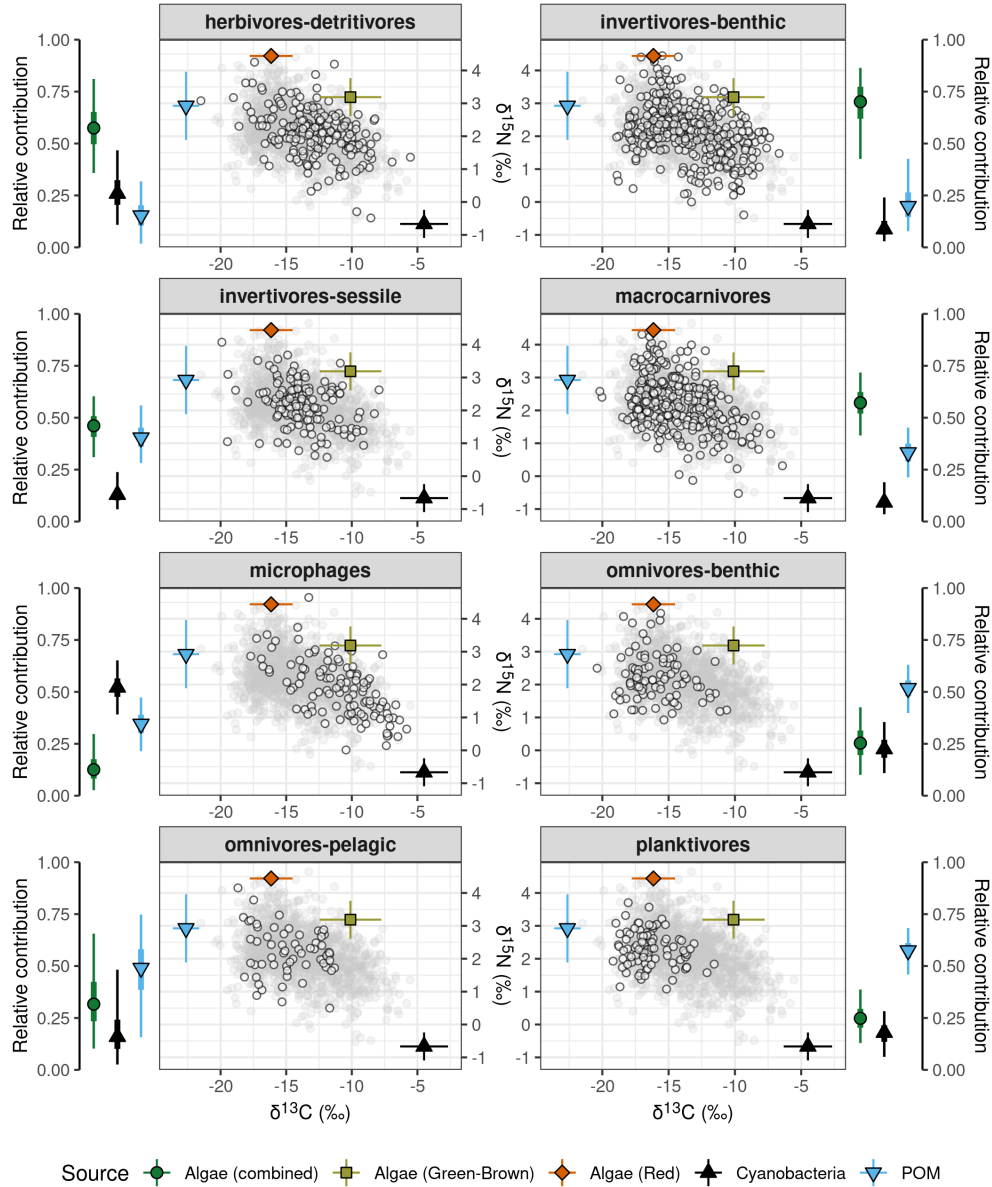


Figure 5: Isospace of reef fish species from Mo’orea, French Polynesia, and relative contribution of basal sources to each trophic guild. Within the isospace, grey, semitransparent dots represent individual fish isotopic signatures rescaled using non-tissue-specific trophic discrimination factors (Post, 2002), white dots represent observations belonging to each trophic guild, while coloured dots and lines represent means ($\pm 1\text{SD}$) isotopic signatures of basal sources. Dots and intervals in side plots represent the median, 50 and 95% credible intervals, respectively, of the estimated relative contribution of basal sources to each trophic guild. Note that the contributions of green-brown algae and red algae were aggregated *a posteriori* to provide an overarching algal contribution. POM = particulate organic matter.

511 4 Discussion

512 We present a comprehensive description of the analytical workflow for estimating consumer
513 reliance on basal food sources using bulk SIA. To our knowledge, existing guidance on this
514 approach is scarce and fragmented. In particular, only brief mentions exist about correcting
515 consumer isotopic values for total trophic discrimination by multiplying the TDF of a single
516 trophic step by the number of trophic steps between the consumer and basal sources (Phillips
517 et al., 2014). Here we make this rationale explicit by describing each step required to derive
518 consumer reliance on basal sources from the bulk stable isotope data. We also test how
519 relaxing some sampling and parameter assumptions influence the results, providing a clear
520 mathematical and empirical foundation for best practices in the analysis of bulk isotope
521 data.

522 We show that the method used to estimate consumer trophic position influences the
523 results (Letourneur et al., 2024), but not to the extent that we anticipated. In particular,
524 we focus on using existing models (Post, 2002) that require a single isotopic baseline, typi-
525 cally using the average $\delta^{15}\text{N}$ of basal sources (e.g., Ferger et al., 2013; Garcia et al., 2018;
526 Moustaka et al., 2024) to represent an average trophic pathway, or two isotopic baselines
527 representing two distinct trophic pathways (e.g., McMahon et al., 2021). Our simulations
528 show that estimates of source-specific reliance for consumers are largely robust to the choice
529 between these two approaches. However, different outcomes could occur on a case-by-case
530 basis, particularly depending on the geometry of the mixing polygon and the position of
531 the consumers in isospace. Indeed, using the average $\delta^{15}\text{N}$ of the basal sources as the sole
532 isotopic baseline will only yield an accurate estimate of trophic position for consumers that
533 uniformly rely on basal sources or primarily on a basal source with an average $\delta^{15}\text{N}$ value.
534 However, as suggested by Equation S10 in Appendix S7, it will overestimate the trophic
535 position of consumers that primarily rely on a basal source with a high $\delta^{15}\text{N}$ value and un-
536 derestimate the trophic position of consumers that primarily rely on a basal source with a
537 low $\delta^{15}\text{N}$ value. Furthermore, this error will be greater as the range in $\delta^{15}\text{N}$ of the sources
538 increases. On the other hand, using two isotopic baselines will yield an accurate estimate of
539 trophic position for consumers that primarily rely on one or more basal sources represented

540 by these baselines, but it may yield an inaccurate estimate for consumers that primarily rely
541 on a basal source not represented by either of the baselines.

542 Nevertheless, our simulations highlight the high sensitivity of the estimated basal source
543 proportions to error in estimating consumer trophic position, indicating that trophic position
544 estimation is a critical step in the workflow. Therefore, while we cannot directly recommend
545 whether to use one or two baselines, we provide an R function (*estimate_tp_error()*, Ap-
546 pendix S8) that implements the equations derived in Appendix S7, which ecologists can use
547 to assess bias in estimating trophic position for hypothetical consumers, given the mean
548 isotopic signature of the sources and baselines. We recommend publishing the expected bias
549 to allow the reader to independently assess the accuracy of the results.

550 Applying this function to our case study, we show that the absolute bias in estimating
551 consumer trophic position is consistently below 0.5 for a set of consumers that primarily rely
552 on one, two, or three basal sources, or equally on all four basal sources (Appendix S5: Tables
553 S7-S8). Furthermore, according to our model (Figure 2), the expected absolute error in the
554 estimated source proportions is consistently less than 0.2, supporting our results.

555 Our simulations also show that consumer and source sample sizes only have a minimal
556 effect on the accuracy of estimated proportions, but larger sample sizes increase the precision
557 of estimates and reduce their uncertainty. Whenever possible, a minimum sample size of ten
558 for each consumer and basal source is recommended. However, under financial constraints or
559 when using pre-existing data, smaller sample sizes may still provide accurate results at the
560 expense of greater uncertainty, while broadening the study scope by allowing for the analysis
561 of a greater number of taxa, locations, or time points.

562 Finally, our case study highlights the sensitivity of the estimated basal source proportions
563 to the choice of isotope-specific TDFs. It is therefore essential to perform a sensitivity analysis
564 using alternative TDFs to increase the robustness of the results and support TDF choices.

565 To facilitate the application of the proposed analytical workflow, we also provide a step-
566 by-step guide in R using a simulated food web in a determined system characterised by
567 three basal sources and two isotopes (Appendix S9). In this vignette, we demonstrate that
568 accurate results can be obtained for 20 simulated species belonging to five families, even
569 with sample sizes as small as one.

570 4.1 Limitations and future directions

571 Our proposed analytical workflow has the following limitations:

- 572 1. Currently available software packages only allow estimation of consumer trophic posi-
573 tion using one or two isotopic baselines, which results in a quantifiable error in trophic
574 position estimates when the studied system has more than two basal sources (Ap-
575 pendix S7). This is typical in complex ecosystems and affects estimates of basal source
576 proportions (Figure 2).
- 577 2. Uncertainty in TDFs and trophic position cannot be propagated into rescaled con-
578 sumer values, as current Bayesian SIMMs do not account for measurement error in
579 individual-level consumer isotopic signatures. This affects the estimated uncertainty
580 in basal source proportions. An alternative approach involves fitting SIMMs according
581 to Equation 5, thus using consumer data at the original scale and incorporating total
582 discrimination and its uncertainty into the model. However, consumer taxa exhibit dis-
583 tinct total discrimination depending on their trophic position. Therefore, a separate
584 SIMM needs to be run for each consumer (e.g., Zapata-Hernández et al., 2021) since
585 it is not currently possible to specify TDFs per factor. While this approach may be
586 preferable in studies involving one or a few taxa, it becomes unrealistic across a larger
587 number of taxa, as in our case study. It can also lead to inefficient inferences with
588 greater uncertainties in source proportions (see Stock et al., 2018), and it limits the
589 ability to obtain large-scale information (e.g., at the level of trophic guilds or higher
590 taxonomic ranks).
- 591 3. Compounding these structural and software constraints, our framework relies on the
592 assumption of constant trophic discrimination. This is a notable limitation, as it is
593 widely recognised that TDFs vary substantially across taxa, diet and tissue types, and
594 trophic groups (Canseco et al., 2022; Caut et al., 2009; Stephens et al., 2023). While
595 alternative frameworks, such as the “narrowing discrimination” approach (Hussey et
596 al., 2014), offer a compelling way to model variable TDFs across multiple trophic lev-
597 els, their application remains severely constrained by data availability and software

598 limitations. Currently, the only available parameters for narrowing discrimination
599 frameworks are restricted to nitrogen isotopes and fish muscle tissue from the founda-
600 tional study that proposed the framework (Hussey et al., 2014). To address this limi-
601 tation and facilitate the adoption of this approach, we have mathematically integrated
602 the narrowing discrimination framework into our proposed workflow in Appendix S2,
603 providing the full required equations for its implementation. However, applying this
604 advanced theoretical framework to our empirical case study was unfeasible due to the
605 lack of derived parameter data for other stable isotopes (such as carbon), as well as the
606 lack of existing software packages capable of fitting these complex models. Because
607 the total trophic discrimination accumulated between basal sources and high-level con-
608 sumers depends inherently on consumer trophic positions—which must be estimated
609 first to rescale consumer isotopic signatures—the constant TDF approach remains the
610 only viable method at present. We validated the robustness of this choice through
611 a sensitivity analysis on the Mo’orea case study, re-running our complete workflow
612 under alternative constant TDFs (general non-tissue-specific vs muscle tissue-specific
613 values). The final estimated basal source proportions exhibited limited sensitivity to
614 these parameter changes, demonstrating that evaluating model sensitivity via alterna-
615 tive constant TDFs remains a critical, reliable safeguard until software capabilities and
616 empirical meta-analyses expand.

617 To address these issues, SIMMs that can explicitly handle multiple trophic steps are
618 desirable (Heikkinen et al., 2022). However, these can only be applied to simple, well-
619 known food webs. For more complex food webs, which constitute the majority of cases, new
620 models based on Equation 2 are needed. These would extend existing models (Equations 6-
621 11), allowing for the estimation of trophic position along with basal source proportions in
622 situations with more than two basal sources and, possibly, modelling both trophic position
623 and source proportions as a function of covariates. However, to avoid underdetermined
624 systems, these models require the same number of stable isotopes as sources (i.e., a third
625 isotope would be needed for a system with three sources).

626 Beyond providing a robust analytical framework, our case study demonstrates how this
627 integrated workflow can be applied to large, complex datasets to extract ecological insights

628 at multiple taxonomic and functional levels. By bridging existing methodological gaps, this
629 framework unlocks the potential to leverage vast, underutilised repositories of stable isotope
630 data across the published literature (e.g., Berto et al., 2025; Boulêtreau et al., 2025; Shipley
631 et al., 2024), enabling researchers to generate novel meta-analyses and synthesise energy
632 pathways at broad macroecological scales. Furthermore, these findings could be scaled di-
633 rectly to the community level to quantify energy and nutrient fluxes across environmental
634 gradients, map functional biogeography, and predict how ecosystem functioning will respond
635 to changes in primary production sources. Ultimately, this workflow offers a scalable and
636 accessible standard that enhances the comparative power of stable isotope ecology across
637 diverse aquatic and terrestrial biomes.

638 **Author Contributions**

639 Mattia Ghilardi, Renato A. Morais and Valeriano Parravicini conceived and designed the
640 study. Simon J. Brandl, Jordan M. Casey, Alexandre Merciere, Fabien Morat, Nina M. D.
641 Schiettekatte and Valeriano Parravicini collected the data for the case study. Mattia Ghilardi
642 developed the workflow and simulations, performed the analysis and wrote the first draft of
643 the manuscript. All authors contributed critically to the drafts and gave final approval for
644 publication.

645 **Acknowledgements**

646 We thank Samuel Degregori, Titouan Roncin, Gabrielle Martineau, Kailey Bissell, Calvin
647 Quigley, Tommy Norin, Jérémy Carlot, and Pierrick Harnay for assistance with field collec-
648 tions and fish dissections. We thank Jason Vii for support with stable isotope preparation.
649 This work was funded by LabEx “Corail” (projects Nectar and METAREEF; VP, MK, YL),
650 the BNP Paribas Foundation (Reef Services Project; VP), and a Make Our Planet Great
651 Again Postdoctoral Grant (mopga-pdf-0000000144; JMC).

652 **Data and Code Availability statement**

653 Code to reproduce results and figures is available on GitHub for both the simulations (https://github.com/mattiaghilardi/SIMMmultitroph_simulations) and the case study (https://github.com/mattiaghilardi/SIMMmultitroph_case_study), along with the Mo'orea stable
654 isotope dataset.
655
656

657 **References**

- 658 Berto, D., Fanelli, E., Vizzini, S., Rampazzo, F., Da Ros, Z., Noventa, S., Fortibuoni, T.,
659 Antonini, C., Cilluffo, G., Signa, G., Premici, A., Bardelli, R., & Raicevich, S. (2025).
660 ISOMED - a stable ISotope database of MEDiterranean marine food web components.
661 *Scientific Data*, 12(1), 1768. <https://doi.org/10.1038/s41597-025-05981-y>
- 662 Bird, C. S., Veríssimo, A., Magozzi, S., Abrantes, K. G., Aguilar, A., Al-Reasi, H., Barnett,
663 A., Bethea, D. M., Biais, G., Borrell, A., Bouchouca, M., Boyle, M., Brooks, E. J.,
664 Brunnschweiler, J., Bustamante, P., Carlisle, A., Catarino, D., Caut, S., Cherel, Y., ...
665 Trueman, C. N. (2018). A global perspective on the trophic geography of sharks. *Nature*
666 *Ecology & Evolution*, 2(2), 299–305. <https://doi.org/10.1038/s41559-017-0432-z>
- 667 Boulêtreau, S., Vagnon, C., Comte, L., Sagouis, A., Pool, T., Stiling, R. R., Harrod, C.,
668 South, J., McIntosh, A. R., Perga, M.-E., Sánchez-Hernández, J., Roussel, J.-M., Tun-
669 ney, T. D., Jackson, M., Olden, J. D., & Cucherousset, J. (2025). IsoFresh: A global
670 stable isotope database of freshwater food webs. *Knowledge & Management of Aquatic*
671 *Ecosystems*, (426), 15. <https://doi.org/10.1051/kmae/2025010>
- 672 Brett, M. T. (2014). Resource polygon geometry predicts bayesian stable isotope mix-
673 ing model bias. *Marine Ecology Progress Series*, 514, 1–12. [https://doi.org/10.3354/](https://doi.org/10.3354/meps11017)
674 [meps11017](https://doi.org/10.3354/meps11017)
- 675 Bürkner, P.-C. (2017). Brms: An r package for bayesian multilevel models using stan.
676 *Journal of Statistical Software*, 80, 1–28. <https://doi.org/10.18637/jss.v080.i01>
- 677 Cabana, G., & Rasmussen, J. B. (1996). Comparison of aquatic food chains using nitrogen
678 isotopes. *Proceedings of the National Academy of Sciences*, 93(20), 10844–10847. <https://doi.org/10.1073/pnas.93.20.10844>

679 //doi.org/10.1073/pnas.93.20.10844

680 Canseco, J. A., Niklitschek, E. J., & Harrod, C. (2022). Variability in $\delta^{13}\text{C}$ and $\delta^{15}\text{N}$
681 trophic discrimination factors for teleost fishes: A meta-analysis of temperature and
682 dietary effects. *Reviews in Fish Biology and Fisheries*, 32(2), 313–329. [https://doi.org/](https://doi.org/10.1007/s11160-021-09689-1)
683 10.1007/s11160-021-09689-1

684 Caut, S., Angulo, E., & Courchamp, F. (2009). Variation in discrimination factors ($\Delta^{15}\text{N}$ and
685 $\Delta^{13}\text{C}$): The effect of diet isotopic values and applications for diet reconstruction. *Journal*
686 *of Applied Ecology*, 46(2), 443–453. <https://doi.org/10.1111/j.1365-2664.2009.01620.x>

687 Clements, K. D., German, D. P., Piché, J., Tribollet, A., & Choat, J. H. (2017). Integrat-
688 ing ecological roles and trophic diversification on coral reefs: Multiple lines of evidence
689 identify parrotfishes as microphages. *Biological Journal of the Linnean Society*, 120(4),
690 729–751. <https://doi.org/10.1111/bij.12914>

691 DeNiro, M. J., & Epstein, S. (1977). Mechanism of carbon isotope fractionation associ-
692 ated with lipid synthesis. *Science*, 197(4300), 261–263. [https://doi.org/10.1126/science.](https://doi.org/10.1126/science.327543)
693 327543

694 Douma, J. C., & Weedon, J. T. (2019). Analysing continuous proportions in ecology and
695 evolution: A practical introduction to beta and dirichlet regression. *Methods in Ecology*
696 *and Evolution*, 10(9), 1412–1430. <https://doi.org/10.1111/2041-210X.13234>

697 Ferger, S. W., Böhning-Gaese, K., Wilcke, W., Oelmann, Y., & Schleuning, M. (2013).
698 Distinct carbon sources indicate strong differentiation between tropical forest and farm-
699 land bird communities. *Oecologia*, 171(2), 473–486. [https://doi.org/10.1007/s00442-012-](https://doi.org/10.1007/s00442-012-2422-9)
700 2422-9

701 Gabry, J., Češnovar, R., Johnson, A., & Bronder, S. (2024). *Cmdstanr: R interface to*
702 *'CmdStan'*. <https://mc-stan.org/cmdstanr/>

703 Gannes, L. Z., Martínez del Rio, C., & Koch, P. (1998). Natural abundance variations
704 in stable isotopes and their potential uses in animal physiological ecology. *Comparative*
705 *Biochemistry and Physiology Part A: Molecular & Integrative Physiology*, 119(3), 725–737.
706 [https://doi.org/10.1016/S1095-6433\(98\)01016-2](https://doi.org/10.1016/S1095-6433(98)01016-2)

707 Gannes, L. Z., O'Brien, D. M., & Martínez del Rio, C. (1997). Stable isotopes in animal
708 ecology: Assumptions, caveats, and a call for more laboratory experiments. *Ecology*,

709 78(4), 1271–1276. <https://doi.org/10.2307/2265878>

710 Garcia, A. F. S., Santos, M. L., Garcia, A. M., & Vieira, J. P. (2018). Changes in food
711 web structure of fish assemblages along a river-to-ocean transect of a coastal subtropical
712 system. *Marine and Freshwater Research*, 70(3), 402–416. [https://doi.org/10.1071/](https://doi.org/10.1071/MF18212)
713 MF18212

714 Gelman, A., & Rubin, D. B. (1992). Inference from iterative simulation using multiple
715 sequences. *Statistical Science*, 7(4), 457–472. <https://doi.org/10.1214/ss/1177011136>

716 Govan, E., Jackson, A. L., Bearhop, S., Inger, R., Stock, B. C., Semmens, B. X., Ward, E. J.,
717 & Parnell, A. C. (2024). *Cosimmr: An r package for fast fitting of stable isotope mixing*
718 *models with covariates* (arXiv:2408.17230). arXiv. [https://doi.org/10.48550/arXiv.2408.](https://doi.org/10.48550/arXiv.2408.17230)
719 17230

720 Govan, E., Jackson, A. L., Inger, R., Bearhop, S., & Parnell, A. C. (2023). *Simmr: A*
721 *package for fitting stable isotope mixing models in r* (arXiv:2306.07817). arXiv. <https://doi.org/10.48550/arXiv.2306.07817>

722

723 Heikkinen, R., Hämäläinen, H., Kiljunen, M., Kärkkäinen, S., Schilder, J., & Jones, R.
724 I. (2022). A bayesian stable isotope mixing model for coping with multiple isotopes,
725 multiple trophic steps and small sample sizes. *Methods in Ecology and Evolution*, 13(11),
726 2586–2602. <https://doi.org/10.1111/2041-210X.13989>

727 Hilting, A. K., Currin, C. A., & Kosaki, R. K. (2013). Evidence for benthic primary pro-
728 duction support of an apex predator–dominated coral reef food web. *Marine Biology*,
729 160(7), 1681–1695. <https://doi.org/10.1007/s00227-013-2220-x>

730 Hussey, N. E., MacNeil, M. A., McMeans, B. C., Olin, J. A., Dudley, S. F. J., Cliff, G.,
731 Wintner, S. P., Fennessy, S. T., & Fisk, A. T. (2014). Rescaling the trophic structure of
732 marine food webs. *Ecology Letters*, 17(2), 239–250. <https://doi.org/10.1111/ele.12226>

733 Kiljunen, M., Grey, J., Sinisalo, T., Harrod, C., Immonen, H., & Jones, R. I. (2006). A
734 revised model for lipid-normalizing ^{13}C values from aquatic organisms, with implications
735 for isotope mixing models. *Journal of Applied Ecology*, 43(6), 1213–1222. [https://doi.](https://doi.org/10.1111/j.1365-2664.2006.01224.x)
736 org/10.1111/j.1365-2664.2006.01224.x

737 Kjeldgaard, M. K., Hewlett, J. A., & Eubanks, M. D. (2021). Widespread variation in
738 stable isotope trophic position estimates: Patterns, causes, and potential consequences.

739 *Ecological Monographs*, 91(3), e01451. <https://doi.org/10.1002/ecm.1451>

740 Landau, W. M. (2021). The targets r package: A dynamic make-like function-oriented
741 pipeline toolkit for reproducibility and high-performance computing. *Journal of Open*
742 *Source Software*, 6(57), 2959. <https://doi.org/10.21105/joss.02959>

743 Landau, W. M. (2024). *Crew: A distributed worker launcher framework*. [https://CRAN.R-](https://CRAN.R-project.org/package=crew)
744 [project.org/package=crew](https://CRAN.R-project.org/package=crew)

745 Letourneur, Y., Fey, P., Dierking, J., Galzin, R., & Parravicini, V. (2024). Challeng-
746 ing trophic position assessments in complex ecosystems: Calculation method, choice
747 of baseline, trophic enrichment factors, season and feeding guild do matter: A case
748 study from marquesas islands coral reefs. *Ecology and Evolution*, 14(7), e11620. [https:](https://doi.org/10.1002/ece3.11620)
749 [//doi.org/10.1002/ece3.11620](https://doi.org/10.1002/ece3.11620)

750 Lindeman, R. L. (1942). The trophic-dynamic aspect of ecology. *Ecology*, 23(4), 399–417.
751 <https://doi.org/10.2307/1930126>

752 Lorrain, A., Pethybridge, H., Cassar, N., Receveur, A., Allain, V., Bodin, N., Bopp, L., Choy,
753 C. A., Duffy, L., Fry, B., Goñi, N., Graham, B. S., Hobday, A. J., Logan, J. M., Ménard,
754 F., Menkes, C. E., Olson, R. J., Pagendam, D. E., Point, D., ... Young, J. W. (2020).
755 Trends in tuna carbon isotopes suggest global changes in pelagic phytoplankton commu-
756 nities. *Global Change Biology*, 26(2), 458–470. <https://doi.org/10.1111/gcb.14858>

757 Maier, M. J. (2014). *DirichletReg: Dirichlet regression for compositional data in r* (Research
758 Report Series / Department of Statistics and Mathematics 125). WU Vienna Univer-
759 sity of Economics; Business. [https://research.wu.ac.at/ws/portalfiles/portal/17761231/](https://research.wu.ac.at/ws/portalfiles/portal/17761231/Report125.pdf)
760 [Report125.pdf](https://research.wu.ac.at/ws/portalfiles/portal/17761231/Report125.pdf)

761 Martínez del Rio, C., Wolf, N., Carleton, S. A., & Gannes, L. Z. (2009). Isotopic ecology
762 ten years after a call for more laboratory experiments. *Biological Reviews*, 84(1), 91–111.
763 <https://doi.org/10.1111/j.1469-185X.2008.00064.x>

764 McConnaughey, T., & McRoy, C. P. (1979). Food-web structure and the fractionation of
765 carbon isotopes in the bering sea. *Marine Biology*, 53(3), 257–262. [https://doi.org/10.](https://doi.org/10.1007/BF00952434)
766 [1007/BF00952434](https://doi.org/10.1007/BF00952434)

767 McCutchan Jr, J. H., Lewis Jr, W. M., Kendall, C., & McGrath, C. C. (2003). Variation
768 in trophic shift for stable isotope ratios of carbon, nitrogen, and sulfur. *Oikos*, 102(2),

769 378–390. <https://doi.org/10.1034/j.1600-0706.2003.12098.x>

770 McMahon, K. W., Ambrose, W. G., Reynolds, M. J., Johnson, B. J., Whiting, A., & Clough,
771 L. M. (2021). Arctic lagoon and nearshore food webs: Relative contributions of terrestrial
772 organic matter, phytoplankton, and phytobenthos vary with consumer foraging dynamics.
773 *Estuarine, Coastal and Shelf Science*, 257, 107388. [https://doi.org/10.1016/j.ecss.2021.](https://doi.org/10.1016/j.ecss.2021.107388)
774 107388

775 McMahon, K. W., Thorrold, S. R., Houghton, L. A., & Berumen, M. L. (2016). Tracing car-
776 bon flow through coral reef food webs using a compound-specific stable isotope approach.
777 *Oecologia*, 180(3), 809–821. <https://doi.org/10.1007/s00442-015-3475-3>

778 Moustaka, M., Bassett, T. J., Beltran, L., Cuttler, M. V. W., Evans, R. D., Gorman, D.,
779 Grimaldi, C. M., Gruber, R. K., Hyndes, G. A., Kendrick, G. A., Travaglione, N., &
780 Wilson, S. K. (2024). Suspended particulate organic matter supports mesopredatory fish
781 across a tropical seascape. *Ecosystems*, 27(7), 918–936. [https://doi.org/10.1007/s10021-](https://doi.org/10.1007/s10021-024-00929-6)
782 024-00929-6

783 Nielsen, J. M., Clare, E. L., Hayden, B., Brett, M. T., & Kratina, P. (2018). Diet tracing
784 in ecology: Method comparison and selection. *Methods in Ecology and Evolution*, 9(2),
785 278–291. <https://doi.org/10.1111/2041-210X.12869>

786 O'Reilly, C. M., Hecky, R. E., Cohen, A. S., & Plisnier, P.-D. (2002). Interpreting stable
787 isotopes in food webs: Recognizing the role of time averaging at different trophic levels.
788 *Limnology and Oceanography*, 47(1), 306–309. <https://doi.org/10.4319/lo.2002.47.1.0306>

789 Osada, Y., Matsubayashi, J., & Tayasu, I. (2021). Diagnosing underdetermination in stable
790 isotope mixing models. *PLOS ONE*, 16(10), e0257818. [https://doi.org/10.1371/journal.](https://doi.org/10.1371/journal.pone.0257818)
791 pone.0257818

792 Parravicini, V., Casey, J. M., Schiettekatte, N. M. D., Brandl, S. J., Pozas-Schacre, C.,
793 Carlot, J., Edgar, G. J., Graham, N. A. J., Harmelin-Vivien, M., Kulbicki, M., Strona,
794 G., & Stuart-Smith, R. D. (2020). Delineating reef fish trophic guilds with global gut
795 content data synthesis and phylogeny. *PLOS Biology*, 18(12), e3000702. [https://doi.org/](https://doi.org/10.1371/journal.pbio.3000702)
796 10.1371/journal.pbio.3000702

797 Pethybridge, H., Choy, C. A., Logan, J. M., Allain, V., Lorrain, A., Bodin, N., Somes, C.
798 J., Young, J., Ménard, F., Langlais, C., Duffy, L., Hobday, A. J., Kuhnert, P., Fry, B.,

799 Menkes, C., & Olson, R. J. (2018). A global meta-analysis of marine predator nitrogen
800 stable isotopes: Relationships between trophic structure and environmental conditions.
801 *Global Ecology and Biogeography*, *27*(9), 1043–1055. <https://doi.org/10.1111/geb.12763>

802 Phillips, D. L., Inger, R., Bearhop, S., Jackson, A. L., Moore, J. W., Parnell, A. C., Semmens,
803 B. X., & Ward, E. J. (2014). Best practices for use of stable isotope mixing models in food-
804 web studies. *Canadian Journal of Zoology*, *92*(10), 823–835. [https://doi.org/10.1139/cjz-](https://doi.org/10.1139/cjz-2014-0127)
805 [2014-0127](https://doi.org/10.1139/cjz-2014-0127)

806 Phillips, D. L., Newsome, S. D., & Gregg, J. W. (2005). Combining sources in stable isotope
807 mixing models: Alternative methods. *Oecologia*, *144*(4), 520–527. [https://doi.org/10.](https://doi.org/10.1007/s00442-004-1816-8)
808 [1007/s00442-004-1816-8](https://doi.org/10.1007/s00442-004-1816-8)

809 Pickett, P. J., Dwyer, G. K., Macqueen, A., Holt, G., Halliday, B. T., Barton, J. L., & Lester,
810 R. E. (2024). Using biotracer techniques to uncover consumer diets: A comparison of
811 stable isotopes, fatty acids, and amino acids. *Ecosphere*, *15*(2), e4767. [https://doi.org/](https://doi.org/10.1002/ecs2.4767)
812 [10.1002/ecs2.4767](https://doi.org/10.1002/ecs2.4767)

813 Plummer, M. (2003). JAGS: A program for analysis of bayesian graphical models using
814 gibbs sampling. *Proceedings of the 3rd International Workshop on Distributed Statistical*
815 *Computing*.

816 Post, D. M. (2002). Using stable isotopes to estimate trophic position: Models, methods,
817 and assumptions. *Ecology*, *83*(3), 703–718. [https://doi.org/10.1890/0012-9658\(2002\)](https://doi.org/10.1890/0012-9658(2002)083%5B0703:USITET%5D2.0.CO;2)
818 [083%5B0703:USITET%5D2.0.CO;2](https://doi.org/10.1890/0012-9658(2002)083%5B0703:USITET%5D2.0.CO;2)

819 Post, D. M., Layman, C. A., Arrington, D. A., Takimoto, G., Quattrochi, J., & Montaña,
820 C. G. (2007). Getting to the fat of the matter: Models, methods and assumptions
821 for dealing with lipids in stable isotope analyses. *Oecologia*, *152*(1), 179–189. [https:](https://doi.org/10.1007/s00442-006-0630-x)
822 [//doi.org/10.1007/s00442-006-0630-x](https://doi.org/10.1007/s00442-006-0630-x)

823 Quezada-Romegialli, C., Jackson, A. L., Hayden, B., Kahilainen, K. K., Lopes, C., & Harrod,
824 C. (2018). tRophicPosition, an r package for the bayesian estimation of trophic position
825 from consumer stable isotope ratios. *Methods in Ecology and Evolution*, *9*(6), 1592–1599.
826 <https://doi.org/10.1111/2041-210X.13009>

827 R Core Team. (2024). *R: A language and environment for statistical computing*. R Founda-
828 tion for Statistical Computing. <https://www.R-project.org/>

829 Reid, D. J., Quinn, G. P., Lake, P. S., & Reich, P. (2008). Terrestrial detritus supports the
830 food webs in lowland intermittent streams of south-eastern australia: A stable isotope
831 study. *Freshwater Biology*, *53*(10), 2036–2050. [https://doi.org/10.1111/j.1365-2427.2008.](https://doi.org/10.1111/j.1365-2427.2008.02025.x)
832 02025.x

833 Rennie, N. (2023). *Ggflowchart: Flowcharts with 'ggplot2'*. [https://nrennie.github.io/](https://nrennie.github.io/ggflowchart/)
834 ggflowchart/

835 Santos, E. P., Condini, M. V., Santos, A. C. A., Alvarez, H. M., Moraes, L. E. de, Garcia, A.
836 F. S., & Garcia, A. M. (2020). Spatio-temporal changes in basal food source assimilation
837 by fish assemblages in a large tropical bay in the SW atlantic ocean. *Estuaries and*
838 *Coasts*, *43*(4), 894–908. <https://doi.org/10.1007/s12237-020-00716-1>

839 Schwarcz, H. P. (1991). Some theoretical aspects of isotope paleodiet studies. *Journal of*
840 *Archaeological Science*, *18*(3), 261–275. [https://doi.org/10.1016/0305-4403\(91\)90065-W](https://doi.org/10.1016/0305-4403(91)90065-W)

841 Semmens, B. X., Ward, E. J., Moore, J. W., & Darimont, C. T. (2009). Quantifying inter-
842 and intra-population niche variability using hierarchical bayesian stable isotope mixing
843 models. *PLOS ONE*, *4*(7), e6187. <https://doi.org/10.1371/journal.pone.0006187>

844 Shipley, O. N., Dabrowski, A. J., Bowen, G. J., Hayden, B., Pauli, J. N., Jordan, C.,
845 Anderson, L., Bailey, A., Bataille, C. P., Cicero, C., Close, H. G., Cook, C., Cook,
846 J. A., Desai, A. R., Evaristo, J., Filley, T. R., France, C. A. M., Jackson, A. L.,
847 Kim, S. L., ... Newsome, S. D. (2024). Design, development, and implementation of
848 IsoBank: A centralized repository for isotopic data. *PLOS ONE*, *19*(9), e0295662.
849 <https://doi.org/10.1371/journal.pone.0295662>

850 Skinner, M. M., Martin, A. A., & Moore, B. C. (2016). Is lipid correction necessary in
851 the stable isotope analysis of fish tissues? *Rapid Communications in Mass Spectrometry*,
852 *30*(7), 881–889. <https://doi.org/10.1002/rcm.7480>

853 Smith, J. A., Mazumder, D., Suthers, I. M., & Taylor, M. D. (2013). To fit or not to fit:
854 Evaluating stable isotope mixing models using simulated mixing polygons. *Methods in*
855 *Ecology and Evolution*, *4*(7), 612–618. <https://doi.org/10.1111/2041-210X.12048>

856 Smithson, M., & Verkuilen, J. (2006). A better lemon squeezer? Maximum-likelihood re-
857 gression with beta-distributed dependent variables. *Psychological Methods*, *11*(1), 54–71.
858 <https://doi.org/10.1037/1082-989X.11.1.54>

859 Solomon, C. T., Carpenter, S. R., Clayton, M. K., Cole, J. J., Coloso, J. J., Pace, M. L.,
860 Vander Zanden, M. J., & Weidel, B. C. (2011). Terrestrial, benthic, and pelagic resource
861 use in lakes: Results from a three-isotope bayesian mixing model. *Ecology*, *92*(5), 1115–
862 1125. <https://doi.org/10.1890/10-1185.1>

863 Stan Development Team. (2024). *Stan reference manual*. <https://mc-stan.org>

864 Stephens, R. B., Shipley, O. N., & Moll, R. J. (2023). Meta-analysis and critical review
865 of trophic discrimination factors ($\Delta^{13}\text{C}$ and $\Delta^{15}\text{N}$): Importance of tissue, trophic level
866 and diet source. *Functional Ecology*, *37*(9), 2535–2548. [https://doi.org/10.1111/1365-](https://doi.org/10.1111/1365-2435.14403)
867 [2435.14403](https://doi.org/10.1111/1365-2435.14403)

868 Stock, B. C., Jackson, A. L., Ward, E. J., Parnell, A. C., Phillips, D. L., & Semmens, B.
869 X. (2018). Analyzing mixing systems using a new generation of bayesian tracer mixing
870 models. *PeerJ*, *6*, e5096. <https://doi.org/10.7717/peerj.5096>

871 Stock, B. C., & Semmens, B. X. (2016). Unifying error structures in commonly used biotracer
872 mixing models. *Ecology*, *97*(10), 2562–2569. <https://doi.org/10.1002/ecy.1517>

873 Ushey, K., & Wickham, H. (2024). *Renv: Project environments*. [https://CRAN.R-project.](https://CRAN.R-project.org/package=renv)
874 [org/package=renv](https://CRAN.R-project.org/package=renv)

875 Vander Zanden, M. J., & Rasmussen, J. B. (1999). Primary consumer $\delta^{13}\text{C}$ and $\delta^{15}\text{N}$ and
876 the trophic position of aquatic consumers. *Ecology*, *80*(4), 1395–1404. [https://doi.org/](https://doi.org/10.1890/0012-9658(1999)080%5B1395:PCCANA%5D2.0.CO;2)
877 [10.1890/0012-9658\(1999\)080%5B1395:PCCANA%5D2.0.CO;2](https://doi.org/10.1890/0012-9658(1999)080%5B1395:PCCANA%5D2.0.CO;2)

878 Vander Zanden, M. J., & Rasmussen, J. B. (2001). Variation in $\delta^{15}\text{N}$ and $\delta^{13}\text{C}$ trophic
879 fractionation: Implications for aquatic food web studies. *Limnology and Oceanography*,
880 *46*(8), 2061–2066. <https://doi.org/10.4319/lo.2001.46.8.2061>

881 Vane, K., Cobain, M. R. D., & Larsen, T. (2025). The power and pitfalls of amino acid carbon
882 stable isotopes for tracing origin and use of basal resources in food webs. *Ecological*
883 *Monographs*, *95*(1), e1647. <https://doi.org/10.1002/ecm.1647>

884 Vehtari, A., Gelman, A., & Gabry, J. (2017). Practical bayesian model evaluation using
885 leave-one-out cross-validation and WAIC. *Statistics and Computing*, *27*(5), 1413–1432.
886 <https://doi.org/10.1007/s11222-016-9696-4>

887 Yao, Y., Vehtari, A., Simpson, D., & Gelman, A. (2018). Using stacking to average bayesian
888 predictive distributions (with discussion). *Bayesian Analysis*, *13*(3), 917–1007. <https://doi.org/10.1214/18-BA1007>

889 //doi.org/10.1214/17-BA1091

890 Zapata-Hernández, G., Sellanes, J., Letourneur, Y., Harrod, C., Morales, N. A., Plaza, P.,
891 Meerhoff, E., Yannicelli, B., Carrasco, S. A., Hinojosa, I., & Gaymer, C. F. (2021). Trac-
892 ing trophic pathways through the marine ecosystem of rapa nui (easter island). *Aquatic*
893 *Conservation: Marine and Freshwater Ecosystems*, 31(2), 304–323. [https://doi.org/10.](https://doi.org/10.1002/aqc.3500)
894 1002/aqc.3500